

Conf-911079--9

EGG- M-91501
PREPRINT

EGG-M--91501

DE92 003308



**Idaho
National
Engineering
Laboratory**

**CALCULATION OF FUEL PIN FAILURE
TIMING UNDER LOCA CONDITIONS**

K. R. Jones, N. L. Wade, L. J. Siefken,
K. R. Katsma, M. Straka

October, 1991

19th Water Reactor Safety Information
Meeting, Bethesda, MD, October 28-30, 1991

This is a preprint of a paper intended for publication in a journal or proceedings. Since changes may be made before publication, this preprint is made available with the understanding that it will not be cited or reproduced without permission of the author.

This report was prepared as an account of work sponsored by an agency of the United States Government. Neither the United States Government nor any agency thereof, or any of their employees, makes any warranty, expressed or implied, or assumes any legal liability or responsibility for any third party's use, or the results of such use, of any information, apparatus, product or process disclosed in this report, or represents that its use by such third party would not infringe privately owned rights. The views expressed in this paper are not necessarily those of the U.S. Nuclear Regulatory Commission.



NOV 25 1991

MASTER

DISTRIBUTION OF THIS DOCUMENT IS UNLIMITED

CALCULATION OF FUEL PIN FAILURE TIMING UNDER LOCA CONDITIONS^a

K. R. Jones, N. L. Wade, L. J. Siefken, M. Straka, K. R. Katsma

ABSTRACT

The objective of this research was to develop and demonstrate a methodology for calculation of the time interval between receipt of the containment isolation signals and the first fuel pin failure for loss-of-coolant accidents (LOCAs). Demonstration calculations were performed for a Babcock and Wilcox (B&W) design (Oconee) and a Westinghouse (W) 4-loop design (Seabrook). Sensitivity studies were performed to assess the impacts of fuel pin burnup, axial peaking factor, break size, emergency core cooling system (ECCS) availability, and main coolant pump trip on these times. The analysis was performed using a four-code approach, comprised of FRAPCON-2, SCDAP/RELAP5/MOD3, TRAC-PF1/MOD1, and FRAP-T6. In addition to the calculation of timing results, this analysis provided a comparison of the capabilities of SCDAP/RELAP5/MOD3 with TRAC-PF1/MOD1 for large-break LOCA analysis. This paper discusses the methodology employed and the code development efforts required to implement the methodology.

The shortest time intervals calculated between initiation of containment isolation and fuel pin failure were 11.4 s and 19.1 s for the B&W and W plants, respectively. The FRAP-T6 fuel pin failure times calculated using thermal-hydraulic data generated by SCDAP/RELAP5/MOD3 were more conservative (earlier) than those calculated using data generated by TRAC-PF1/MOD1.

1. INTRODUCTION

A licensing basis for nuclear reactors has been the loss-of-coolant accident (LOCA), with an assumed instantaneous release of fission products from the fuel into the containment. Certain equipment performance requirements, such as rapid closure of containment isolation valves, have been required to facilitate compliance with 10 CFR Part 100¹ regarding offsite radiological consequences. These fast closure times have placed a burden on valve design and maintenance.

The objective of this research was to develop a viable methodology for

a. Work supported by the U.S. Nuclear Regulatory Commission, Office of Nuclear Regulatory Research, under DOE Contract No. DE-AC07-76ID01570.

calculation of the timing of the earliest fuel pin cladding failure, relative to the containment isolation signal, for LOCAs. The calculation was expected to show that certain isolation valves do not have to be closed as rapidly as now required, thus permitting more realistic licensing requirements.

In order to meet this objective, a calculational methodology was developed employing the FRAPCON-2², SCDAP/RELAP5/MOD3³, and FRAP-T6⁴ computer codes. Demonstration calculations were performed, applying this methodology to two plant designs, a Babcock and Wilcox (B&W) design analyzed using an Oconee plant model and a Westinghouse (W) 4-loop design analyzed using a Seabrook plant model. Sensitivity studies were performed involving varied break sizes, fuel pin burnups, and axial peaking factors.

These calculations represent the first application of SCDAP/RELAP5/MOD3 and were performed using a preliminary version of the code, prior to completion of the code assessment efforts. In order to evaluate the adequacy of SCDAP/RELAP5/MOD3, a single TRAC-PF1/MOD1⁵ calculation was performed, duplicating the worst-case SCDAP/RELAP5/MOD3 calculation for the Seabrook analysis. This calculation consisted of a complete, double-ended, offset-shear break of a cold leg, without pumped emergency core cooling systems (ECCS) and assuming that the main coolant pumps continued operating.

This paper summarizes the methodology developed for these calculations and the results obtained from two demonstration calculations.

2. METHODOLOGY

A four-code approach, utilizing FRAPCON-2, SCDAP/RELAP5/MOD3, TRAC-PF1/MOD1, and FRAP-T6, was adopted for the analysis. This approach provided a defensible calculational methodology for performing the analyses, incorporating a fully assessed calculational path, using FRAPCON-2, TRAC-PF1/MOD1, and FRAP-T6, and a parallel path, utilizing FRAPCON-2, SCDAP/RELAP5/MOD3, and FRAP-T6.

The FRAPCON-2² code was developed to calculate the steady-state response of light water reactor (LWR) fuel rods during long-term burnup. It calculates the temperature, pressure, deformation, and failure histories of a fuel rod as functions of time-dependent fuel rod power and coolant boundary conditions.

The FRAP-T6⁴ code was developed to predict the performance of LWR fuel rods during operational transients and hypothetical accidents. It obtains initial fuel rod conditions by reading a file created by the FRAPCON-2 code and calculates all of the phenomena that influence the transient performance of fuel rods, with particular emphasis on temperature and deformation of the cladding.

Both FRAPCON-2 and FRAP-T6 have been thoroughly assessed over a range of normal burnups;⁶⁻⁹ however, they have not been assessed for analysis of high-burnup fuel (>35 GWd/MTU). Results obtained for exposures above 35 GWd/MTU are in general agreement with expected trends. In addition, it is not anticipated

that high-burnup fuel pins (>35 GWd/MTU) would be operating at power levels that would cause them to fail earlier than lower-burnup pins.

The SCDAP/RELAP5/MOD3³ code was developed for best-estimate transient simulation of LWR coolant systems under severe accident conditions, as well as large- and small-break LOCAs. It is currently under development, and a preliminary version (cycle 7B) was used for the analyses.

The TRAC-PF1/MOD1 code⁵ was developed for transient simulation of LWR coolant systems during large-break LOCAs. Version 14.3U5Q.LG was used for this analysis. This version was frozen in 1987 by the U.S. Nuclear Regulatory Commission for use in the code scaling, applicability, and uncertainty evaluation (CSAU) study.¹⁰ A broad assessment effort has been completed, which has demonstrated that the code is capable of addressing the entire large-break LOCA scenario (blowdown, refill, and reflood). Appendix III of the CSAU report¹⁰ provides an extensive list of assessment reports applicable to this code.

SCDAP/RELAP5/MOD3 was chosen as the primary thermal-hydraulic code for the analysis, since it provides a considerable cost savings over TRAC-PF1/MOD1 for calculation of system thermal-hydraulic response under LOCA conditions. SCDAP/RELAP5/MOD3 is a relatively fast-running code that can execute from a workstation platform, as opposed to TRAC-PF1/MOD1, which requires a mainframe platform. A wide range of sensitivity cases were analyzed using SCDAP/RELAP5/MOD3 to assess the impact of break size, ECCS availability, and main coolant pump trip on the fuel failure timing. However, due to the lack of code assessment for SCDAP/RELAP5/MOD3, a supplemental TRAC-PF1/MOD1 calculation, duplicating the case resulting in the shortest time to pin failure, was run to provide an evaluation of its accuracy.

The calculational methodology using SCDAP/RELAP5/MOD3 is illustrated in Figure 1. In these calculations, FRAPCON-2 was used to calculate the burnup-dependent fuel pin initial conditions for FRAP-T6; FRAP-T6 was used to calculate the initial steady-state fuel pin conditions for SCDAP/RELAP5/MOD3; SCDAP/RELAP5/MOD3 was run to obtain the system thermal-hydraulic boundary conditions, consisting of the fuel pin power distribution and thermodynamic conditions of the coolant channel; and FRAP-T6 was used to calculate the transient fuel pin behavior.

The supplemental calculation utilizes a similar methodology with the exception that SCDAP/RELAP5/MOD3 is replaced by TRAC-PF1/MOD1, as illustrated in Figure 2. Initialization of burnup-dependent variables for the TRAC-PF1/MOD1 fuel components is not necessary, since the code does not have a fuel performance model. However, a comparison of initial stored energy calculated by TRAC-PF1/MOD1 to that calculated by FRAP-T6 indicated reasonable agreement.

A significant software development effort was conducted to implement the chosen methodology. This effort included conversion of the FRAPCON-2 and FRAP-T6 codes to portable FORTRAN 77 to allow execution on a 32-bit-based UNIX workstation, and the creation of interface codes to link the thermal-hydraulics codes to FRAP-T6. In addition, advanced graphics capabilities were added to the FRAP-T6 code. These capabilities include interfacing to the Nuclear Plant

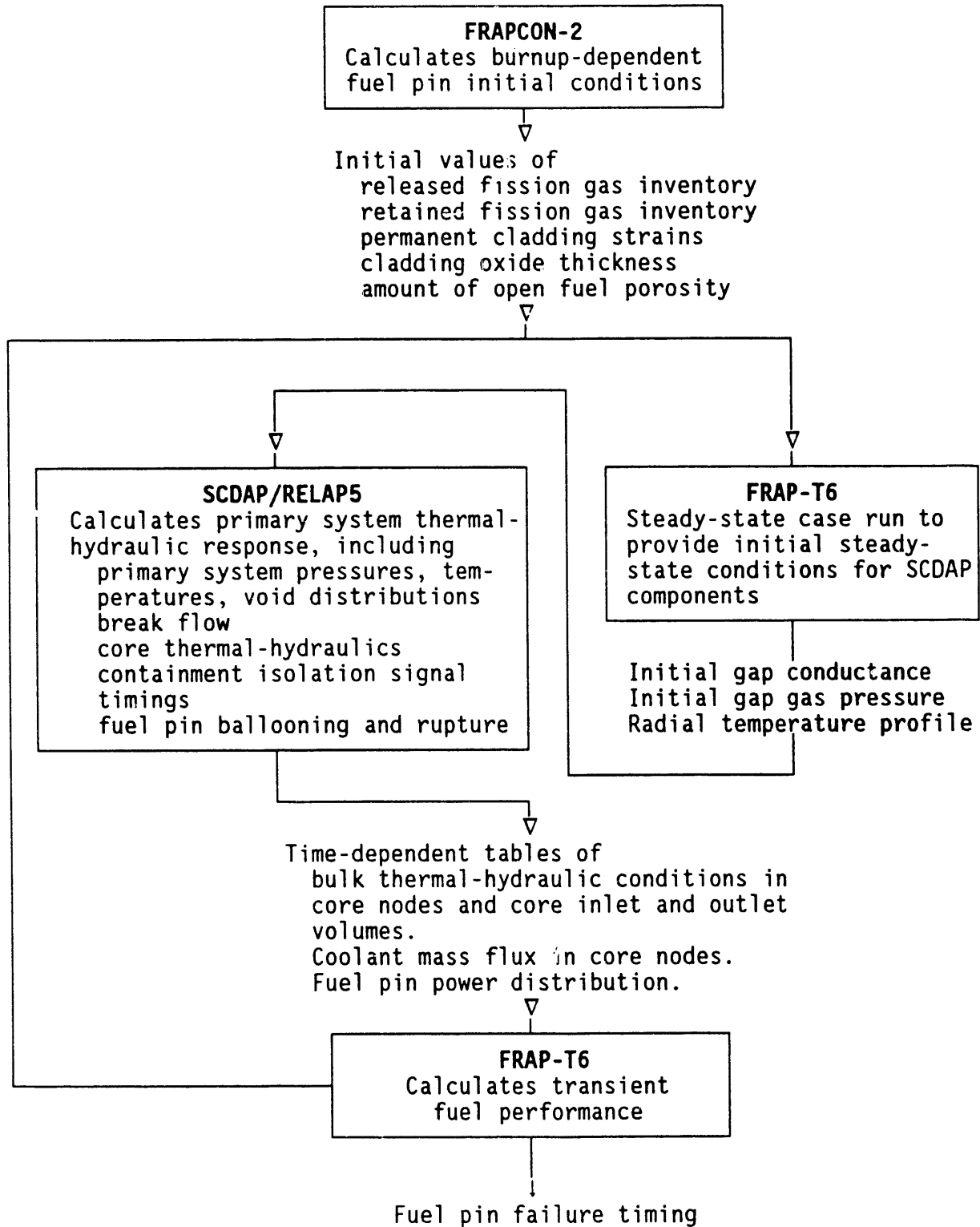


Figure 1. Flow chart of methodology using SCDAP/RELAP5/MOD3 thermal-hydraulic data.

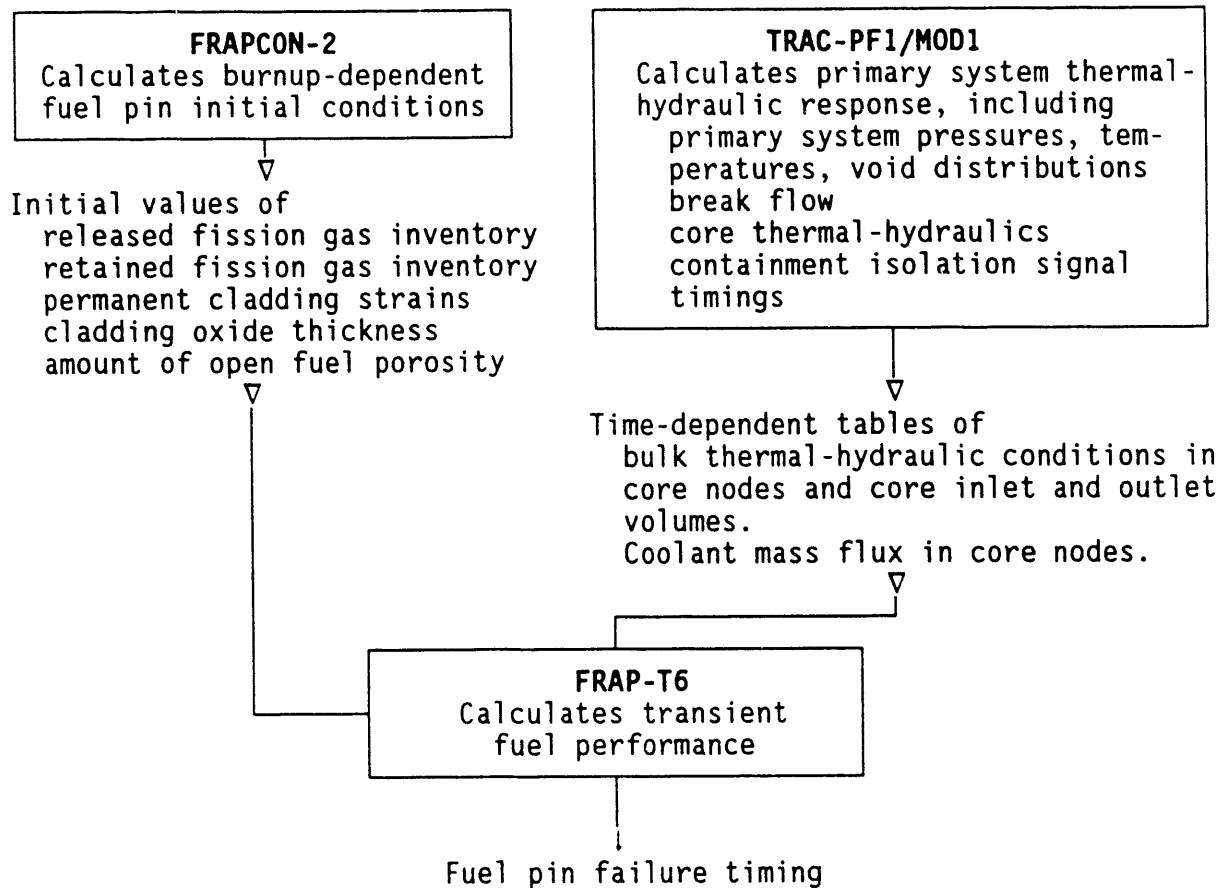


Figure 2. Flow chart of methodology using TRAC-PF1/MOD1 thermal-hydraulic data.

Analyzer (NPA)¹¹ and the GRAFITI¹² graphics packages. The NPA software is an advanced interactive graphics package that provides an animated display of the fuel rod behavior during program execution. The GRAFITI package provides a presentational graphics capability.

3. MODEL DEVELOPMENT

The calculations were performed assuming an equilibrium core operating at 102% core thermal power. Similar core nodalization was used for the SCDAP/RELAP5/MOD3 and TRAC-PF1/MOD1 models, with the exception that the core bypass was lumped into the outer core region in the TRAC-PF1/MOD1 model. This nodalization consisted of a detailed three-channel core model with nine axial nodes, simulating hot channel, central, and outer regions of the core. The hot channel included four fuel assemblies. The total power generated in the hot

channel was assumed to be governed by the technical specification enthalpy rise hot channel factor.

The Seabrook SCDAP/RELAP5/MOD3 model used for this analysis was adapted from a RELAP5/MOD2 deck created for station blackout transient analysis of the Seabrook nuclear power plant.¹³ The Oconee SCDAP/RELAP5/MOD3 model was derived from a RELAP5/MOD2 model created for evaluation of operational safety at B&W plants.¹⁴ Several modifications were required to produce the models needed for this analysis. These included the addition of a detailed 3-channel, 9-axial-node core model, describing the hot channel and the central and outer core region; point kinetics modeling; SCDAP modeling; a simplified containment model; and a detailed downcomer model.

A simplified containment model, consisting of a single RELAP5 volume with heat conductors representing steel and concrete surfaces, provided a fairly rough estimate of containment response. A more detailed treatment of containment response would require the use of a containment analysis code. For Seabrook, results indicate that the containment isolation signal from the pressurizer low pressure trip trails the signal received from high containment pressure by only about 3 s. Due to the approximate nature of the containment pressure calculation, the pressurizer low pressure trip time was used to determine the containment isolation signal time. For Oconee large-break cases, the containment isolation signal from the reactor coolant system (RCS) low pressure trip trails the signal received from high containment pressure by only about 0.02 to 0.28 s; the RCS low pressure trip time was used to determine the containment isolation signal time. For the small-break cases, the high containment pressure trip trails the low RCS pressure trip by about 5 s; the high containment pressure trip was used to determine the time of containment isolation.

The Seabrook TRAC-PF1/MOD1 model used for this analysis was derived from a TRAC-PF1/MOD1 model utilized for the CSAU study.¹⁰ The modifications for this analysis included renodalization of the core region from five to nine axial nodes, describing the hot channel and the central and outer core region, removal of pumped ECCS, modification of the core power distribution, and replacement of containment pressure and decay heat boundary conditions. Boundary conditions for containment pressure and total core power history were obtained from the corresponding SCDAP/RELAP5/MOD3 calculation.

The FRAPCON-2, FRAP-T6, and SCDAP fuel pin models were developed specifically for this analysis. A single fuel pin design was modeled for each plant type analyzed. These fuel designs included the Mk-B9/10 design for the Oconee analysis and the W 17x17 standard fuel design for the Seabrook analysis. Reactor-specific fuel data were obtained either from the fuel vendor or the appropriate Final Safety Analysis Report.^{15,16} The basic design parameters for each fuel type are summarized in Table 1.

The results generated by this analysis are dependent on the specific fuel design parameters, such as initial helium fill inventory, fuel pellet dimensions,

Table 1. Summary of fuel design characteristics

| Characteristic | B&W Mk-B9/10 | W 17x17 standard |
|--|--------------|------------------|
| Pin lattice | 15x15 | 17x17 |
| Fuel pins per assembly | 208 | 264 |
| Fuel pellet OD (in.) | 0.370 | 0.3225 |
| Cladding ID (in.) | 0.377 | 0.329 |
| Cladding OD (in.) | 0.430 | 0.374 |
| Plenum length (in.) | 8.394 | 6.479 |
| Initial fuel stack height (in.) | 140.595 | 144.0 |
| Fuel enrichment (wt. % ²³⁵ U) | 3.5 | 3.1 |

cladding dimensions, and plenum volume. Fuel pin failure times can be expected to vary with both fuel design and reactor design.

4. SENSITIVITY STUDIES

Using SCDAP/RELAP5/MOD3, sensitivity studies were performed for each reactor type to identify the break size resulting in the shortest time to pin failure. The large-break spectrum analyzed consisted of double-ended, offset-shear breaks of a cold leg, with break sizes corresponding to 100%, 90%, 75%, and 50% of the full design basis analysis (DBA) cold leg break area (200% of the cold leg cross-sectional area). For these cases, the break modeling consisted of restarting a steady-state calculation with a percentage of the flow area from each side of a cold leg junction redirected into the containment volume. The junction control flag for an abrupt area change was turned on for each break junction. The break model for the 6-in.-diameter, small-break LOCA consisted of a trip valve located between the cold leg and the containment at the same location used for the large-break case.

The large-break spectrum was run without any pumped ECCS available. The large-break cases resulting in the shortest time to pin failure were also run with pumped ECCS available, to determine the impact of ECCS on pin failure timing. The accumulators were assumed to be available for all cases.

The base analysis did not incorporate a concurrent loss of offsite power. As a result, the reactor coolant pumps are assumed to continue operation throughout the transient. Sensitivity cases were run using the worst-case break size, both with and without pumped ECCS, to determine the impact of tripping the RCS pumps at time zero.

For each set of large-break transient thermal-hydraulic conditions generated by SCDAP/RELAP5/MOD3, a series of 16 FRAP-T6 cases were run to determine fuel pin failure times for a range of fuel pin peak burnups and axial power peaking

factors, up to and including the heat flux hot channel factor. A fundamental assumption governing this methodology is that the hot channel thermal-hydraulic conditions generated by SCDAP/RELAP5/MOD3 do not vary significantly for changes in hot pin axial power profile. In each case, the total fuel pin power, integrated over the length of the pin, is governed by the enthalpy rise hot channel factor and is therefore independent of the axial peaking factor applied.

For each small-break SCDAP/RELAP5/MOD3 calculation, a preliminary matrix of four FRAP-T6 cases was executed. These cases correspond to the highest burnup and peaking factor for each reactor. Since no fuel pin failure was observed prior to 393 s for Oconee and 600 s for Seabrook (at which time code failure was encountered in SCDAP/RELAP5/MOD3), no additional FRAP-T6 cases were run.

FRAP-T6 is a best-estimate code; however, a set of evaluation models, including the NUREG-0630¹⁷ ballooning model, are available as options that can be used to perform calculations of fuel rod behavior that can satisfy most criteria specified in 10 CFR, Part 50, Appendix K.¹⁸ The evaluation models include the areas of mechanical deformation and rupture, thermal-hydraulic boundary conditions, initial conditions, and material properties of fuel and cladding. The 16-case FRAP-T6 matrix was repeated for the worst-case break size (100% DBA) using the evaluation model options.

In addition to the cases described above, the 16-case FRAP-T6 matrix for the worst-case break size for the Seabrook reactor (100% DBA) was run using thermal-hydraulic boundary condition data provided by TRAC-PF1/MOD1.

5. RESULTS

The results of the timing analysis of PWR fuel pin failures are summarized below. Sections 5.1 and 5.2 describe the accident scenarios considered and the fuel pin failure results obtained from FRAP-T6 using thermal-hydraulic boundary conditions calculated by SCDAP/RELAP5/MOD3 and TRAC-PF1/MOD1, respectively.

5.1 RESULTS GENERATED USING SCDAP/RELAP5/MOD3

The thermal-hydraulic results calculated by SCDAP/RELAP5/MOD3 for the worst-case LOCA for Oconee are illustrated in Figure 3. Core thermal power drops off rapidly in response to core voiding. Falling pressurizer pressure lags the drop in system pressure, due to choking in the surge line. Starting at about 30 s, collapsed reactor water level begins a gradual recovery as flow from the accumulators begins to reach the core. The containment isolation trip setpoints were exceeded at 0.6 and 3.7 s for Oconee and Seabrook, respectively. An additional 2-s delay to account for instrument response times was assumed for each plant for calculating the containment isolation times.

The hot channel thermal-hydraulic conditions generated by each

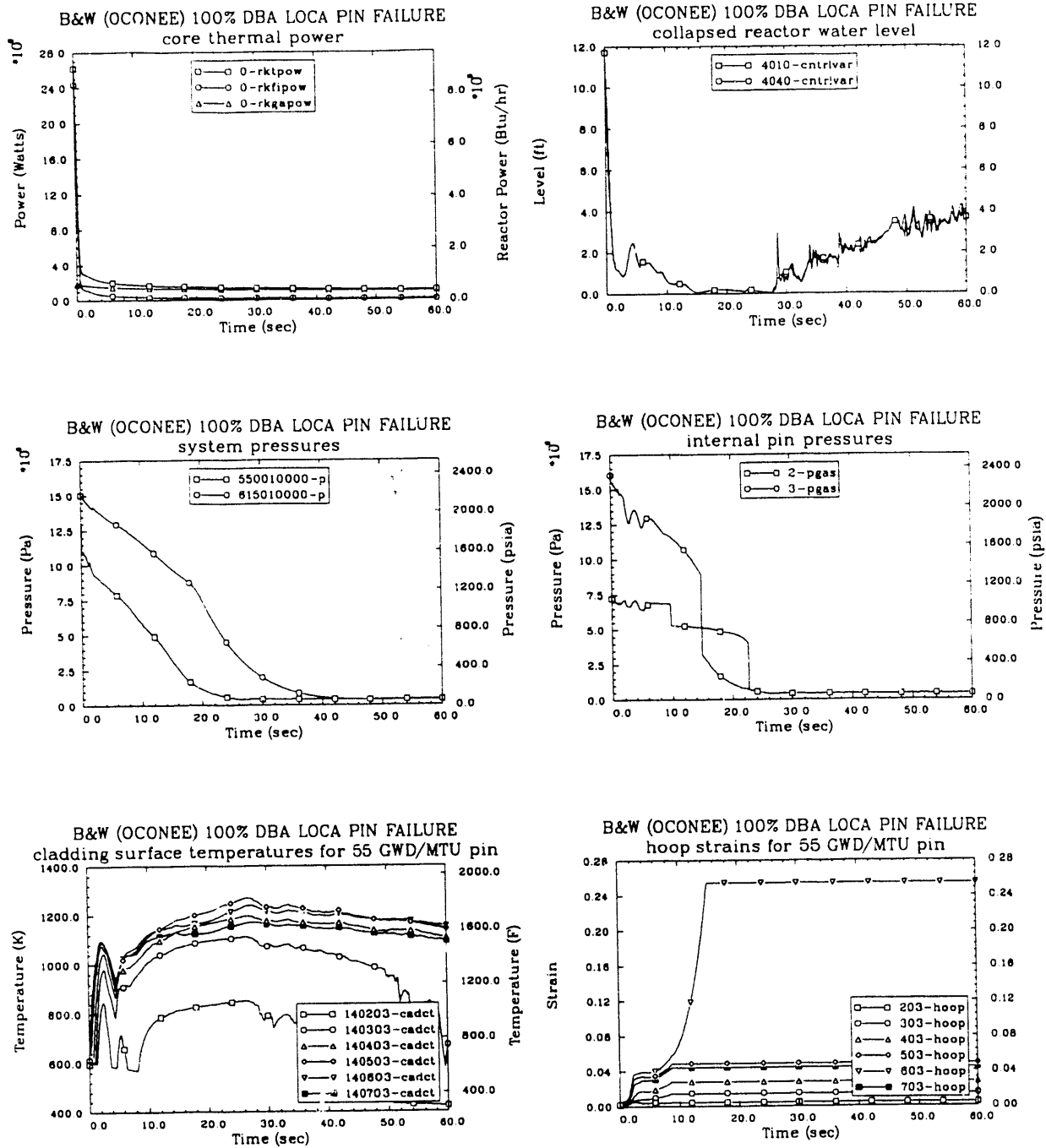
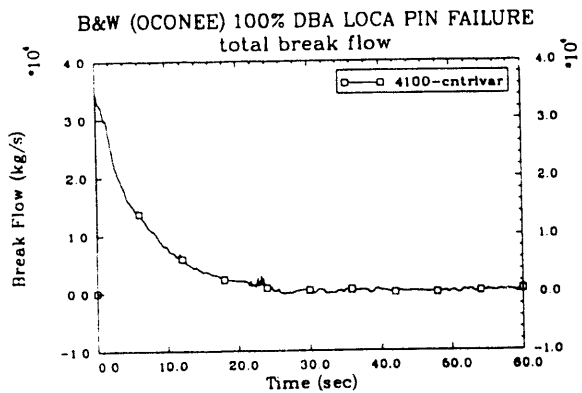


Figure 3. Plots of the transient results generated by SCDAP/RELAP5/MOD3 for a complete double-ended offset shear LOCA for Oconee.



| Variable | Description |
|-------------------------------------|--|
| SCDAP/RELAP5/MOD3 Variables: | |
| 0-rktpow | Total core thermal power (W) |
| 0-rkfipow | Total core fission power (W) |
| 0-rkgapow | Total core decay heat (W) |
| 4010-cntrlvar | Hot channel collapsed reactor water level (m) |
| 4040-cntrlvar | Core-average collapsed reactor water level (m) |
| 550010000-p | Reactor upper head pressure (Pa) |
| 615010000-p | Pressurizer dome pressure (Pa) |
| 2-pgas | Internal pin pressure for 5 GWD/MTU pin (Pa) |
| 3-pgas | Internal pin pressure for 55 GWD/MTU pin (Pa) |
| 14nn01-cadct | High-burnup fuel pin cladding temperature for node nn (°K) |
| nn03-hoop | High-burnup fuel pin cladding hoop strain (dimensionless) |
| 4100-cntrlvar | Total break flow (kg/s) |
| 702000000-mflowj | Total accumulator flow (kg/s) |

Figure 3. (continued)

SCDAP/RELAP5/MOD3 run were used to provide boundary conditions for FRAP-T6, which calculated fuel pin failure times for a matrix of fuel pin exposures and peaking factors. The fuel pin failure times calculated by FRAP-T6 for the worst-case LOCA are summarized in Tables 2 and 3 for Oconee and Seabrook, respectively. In cases where no fuel pin failure was predicted, the values given in the tables correspond to the transient time at the end of the calculation, prefixed by a "greater than" symbol (>). The failure nodes are indicated by the numbers in parentheses; nodes are numbered from 1 at the bottom of the core to 9 at the top.

Table 2. FRAP-T6-calculated hot fuel pin failure time (s) and locations as a function of burnup and peaking factor (pf) for a complete, double-ended, offset-shear LOCA for Oconee.

| Burnup/pf | 5 GWd/MTU | 20 GWd/MTU | 35 GWd/MTU | 55 GWd/MTU |
|-----------|-----------|------------|------------|------------|
| 2.63 | 22.7 (5) | 20.3 (4) | 18.0 (4) | 13.0 (4) |
| 2.4 | > 60.0 | 25.3 (4) | 19.7 (4) | 14.1 (4) |
| 2.2 | > 60.0 | 34.8 (4) | 23.9 (4) | 16.4 (4) |
| 2.0 | > 60.0 | >60.0 | 33.8 (4) | 22.5 (4) |

Table 3. FRAP-T6-calculated hot fuel pin failure time (s) and locations as a function of burnup and peaking factor (pf) for a complete, double-ended, offset-shear LOCA for Seabrook.

| Burnup/pf | 5 GWd/MTU | 20 GWd/MTU | 35 GWd/MTU | 50 GWd/MTU |
|-----------|-----------|------------|------------|------------|
| 2.32 | 29.1 (5) | 29.7 (5) | 27.7 (5) | 24.8 (4) |
| 2.2 | 34.4 (5) | 36.7 (5) | 35.8 (5) | 32.5 (4) |
| 2.0 | 44.5 (4) | 48.4 (4) | 43.6 (4) | 43.6 (4) |
| 1.8 | > 60.0 | > 60.0 | > 60.0 | > 60.0 |

The transient fuel pin performance results calculated by FRAP-T6 are shown in Figures 4 and 5 for Oconee and Seabrook, respectively. Initially, the fuel pin internal pressures drop gradually as the fuel pin plenum temperatures drop and ballooning of the cladding occurs. A sudden drop in fuel pin internal pin pressure to the system pressure is observed when the fuel pin failure criterion (failure probability > 0.5) is reached.

The fuel cladding surface temperatures rise rapidly during the first few seconds, as the fuel rod surface heat flux is reduced due to core voiding. Fuel cladding temperatures peak at about 1100 K, then decline over the next few

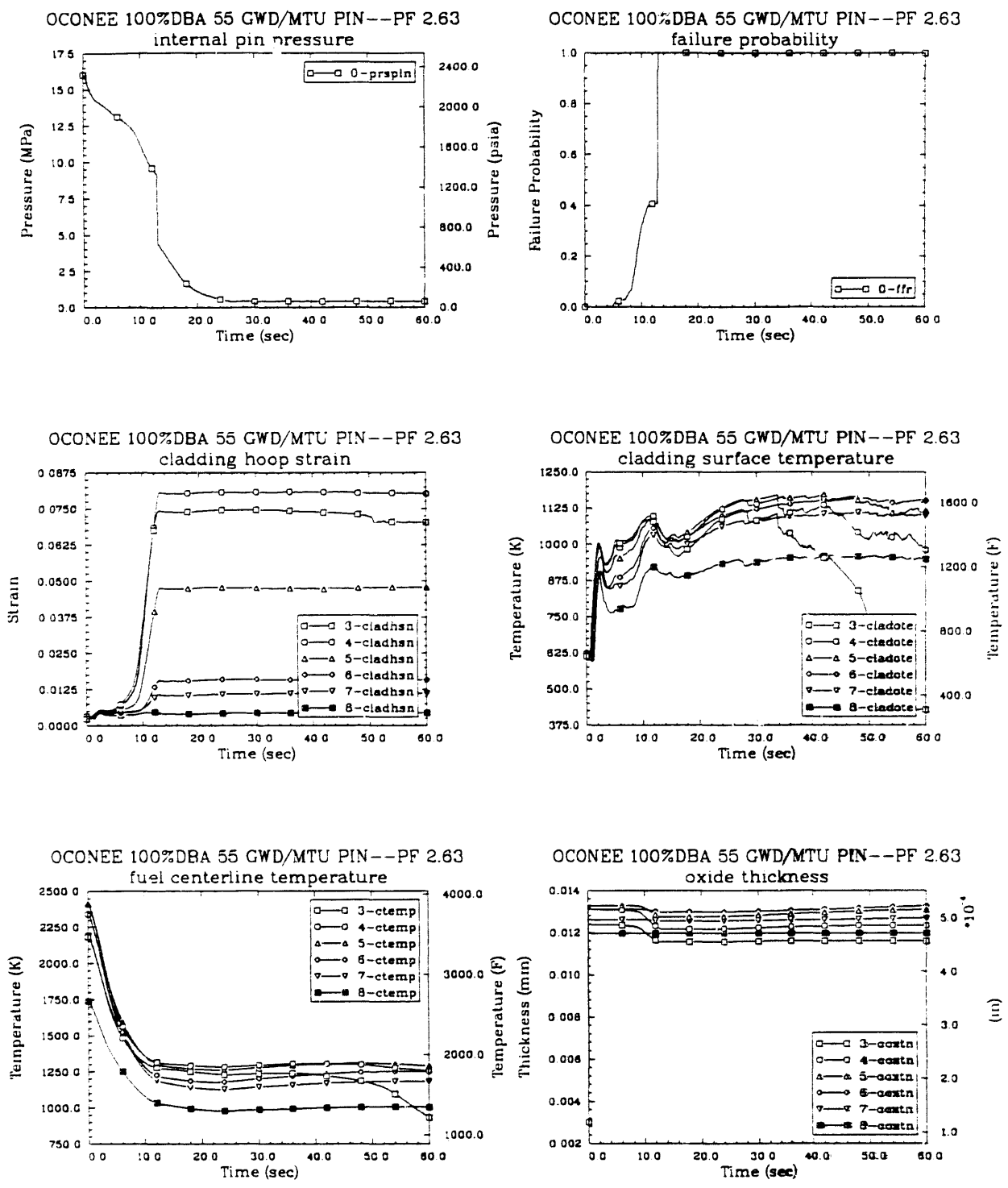
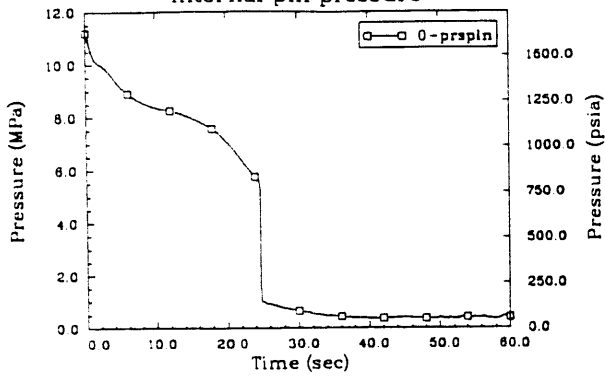
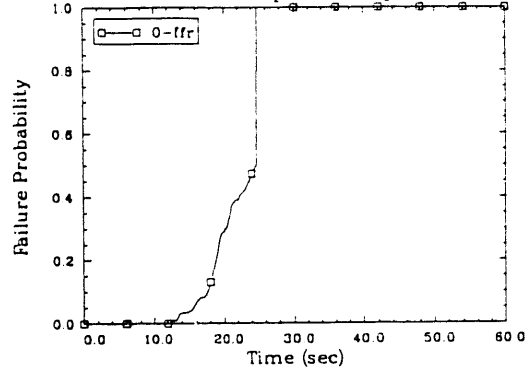


Figure 4. FRAP-T6 transient fuel performance results for an Oconee hot channel hot pin, peaking factor 2.63, 55 GwD/MTU burnup, using SCDAP/RELAP5/MOD3 thermal-hydraulic boundary condition data.

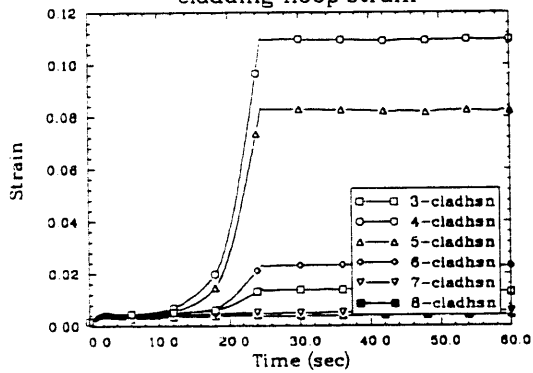
SEABROOK 100%DBA 50 GWD/MTU PIN--PF 2.32
internal pin pressure



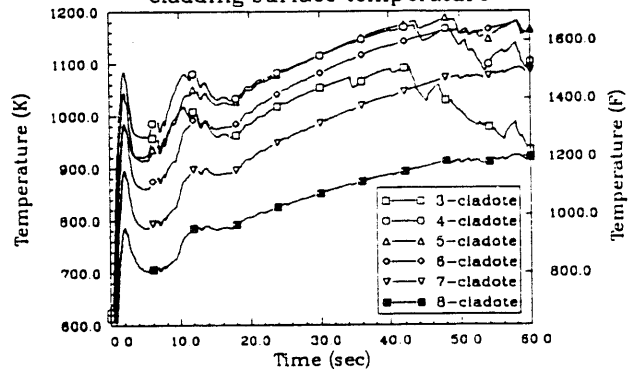
SEABROOK 100%DBA 50 GWD/MTU PIN--PF 2.32
failure probability



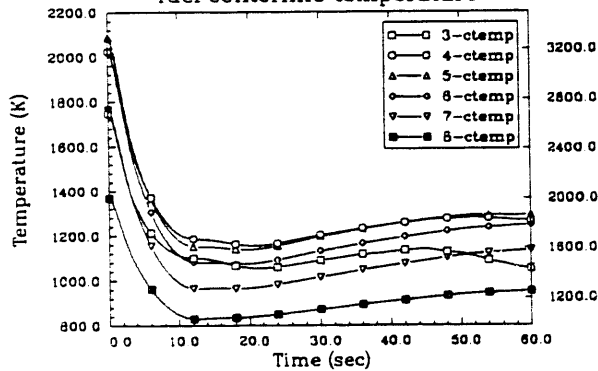
SEABROOK 100%DBA 50 GWD/MTU PIN--PF 2.32
cladding hoop strain



SEABROOK 100%DBA 50 GWD/MTU PIN--PF 2.32
cladding surface temperature



SEABROOK 100%DBA 50 GWD/MTU PIN--PF 2.32
fuel centerline temperature



SEABROOK 100%DBA 50 GWD/MTU PIN--PF 2.32
oxide thickness

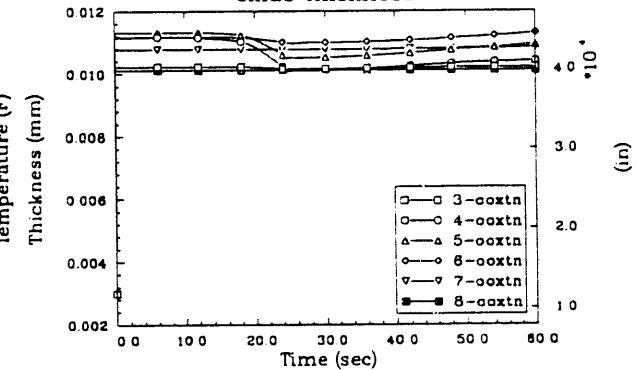


Figure 5. FRAP-T6 transient fuel performance results for a Seabrook hot channel hot pin, peaking factor 2.32, 50 GWD/MTU burnup, using SCDAP/RELAP5/MOD3 thermal-hydraulic boundary condition data.

seconds as the fuel gives up its stored energy and fuel pellet temperatures drop due to the reduced power generation. Eventually, the reduced heat transfer at the cladding surface produces a steady rise in cladding and fuel pellet temperatures. This temperature rise continues until water from the accumulators (and the pumped ECCS, if available) makes its way into the core region.

The zircaloy cladding undergoes a phase change starting at about 1050-1090 K and ending at about 1250 K. As a result of this phase change, the material properties of the cladding change rapidly over this temperature range. In each case, pin failures were calculated to occur during this phase transition prior to reaching a temperature of 1250 K.

The fuel centerline temperatures calculated by SCDAP/RELAP5/MOD3 for both the Oconee and Seabrook models are in fairly close agreement with those calculated by the best-estimate models of FRAP-T6. The Seabrook results also indicate good agreement between SCDAP/RELAP5/MOD3 and FRAP-T6 cladding surface temperatures; however, for Oconee, SCDAP/RELAP5/MOD3 tends to overpredict cladding surface temperatures in comparison to those calculated by FRAP-T6. These differences are attributed to the different heat transfer correlations used in the two codes.

The fuel pin failure times calculated by SCDAP/RELAP5/MOD3 do not, in general, correlate well with those calculated by FRAP-T6. Except for the Oconee 100% DBA LOCA cases, the fuel pin failure times calculated by SCDAP/RELAP5/MOD3 tend to be longer than those calculated by FRAP-T6. This discrepancy increases significantly as the break size is reduced. A fairly good agreement is obtained between the two codes for the 100% DBA Oconee cases, both with and without pumped ECCS. However, fuel pin failure times calculated by SCDAP/RELAP5/MOD3 are about half of those calculated by FRAP-T6 for the two 100% DBA Oconee cases run with main coolant pump trip.

The observed deviations between FRAP-T6 and SCDAP fuel pin failure times can be traced, at least in part, to the difference in the cladding strains calculated by the two codes. In SCDAP, a step change in cladding strain was encountered at each axial node of the low-exposure fuel pins at around 10 s for each large-break LOCA case for both the Oconee and Seabrook fuel pins. This step change in cladding strain was also calculated for the Seabrook high-exposure fuel pin. The cladding deformation model does not appear to be properly taking strain rate effects into account. The step change in cladding strain produces a step decrease in internal fuel pin pressure. As illustrated by the plots of internal pin pressure calculated by SCDAP/RELAP5/MOD3 (see Figure 3), the step decrease in pressure early in the transient results in a delayed time to fuel pin rupture. SCDAP/RELAP5/MOD3 overpredicts the axial extent of cladding deformation, which results in an underprediction of internal pin pressures and an overprediction of the time to fuel pin failure.

The minimum time to fuel pin failure for Oconee, calculated with the FRAP-T6 best-estimate models, is 13.0 s for the 100% DBA case without RCS pump trip. This time was not affected by availability of pumped ECCS. The minimum time to fuel pin failure calculated by FRAP-T6 for Seabrook is 24.6 s for the 100% DBA case without ECCS available. Overall, the results generated by FRAP-T6 are

consistent with expected trends. Pin failure times shortened as peaking factors, burnups, and break areas were increased.

The earliest pin failure times calculated for Oconee are significantly shorter than those calculated for Seabrook. The shorter failure times can be directly attributed to the higher linear heat generation rate and the larger fuel pin diameter in Oconee, which results in higher initial stored energy. In addition, the failure times calculated for Oconee are stronger functions of burnup than those reported for Seabrook. The pin failure times calculated for Seabrook are only weak functions of burnup, with only about 5 s separating the pin failure times over the range of burnups.

Several parameters affecting fuel pin failure times vary as a function of exposure, including cladding creep, fuel and cladding material properties, internal gas pressure, and gap conductance. The fuel pin failure times calculated for Seabrook generally increase between 5 and 20 GWd/MTU and then decrease to the shortest pin failure time at 50 GWd/MTU. The increase in fuel pin failure time between 5 and 20 GWd/MTU can be attributed to the decrease in stored energy over this period, resulting from cladding creep and increased gap conductance. After 20 GWd/MTU, the fuel pin internal pressure becomes the dominant factor affecting the fuel failure timing.

The stored energy calculated for Oconee does not vary with exposure to the same extent as observed in the Seabrook analysis. Fuel pin failure times for Oconee are dominated primarily by the internal pin pressure, resulting in a stronger dependence on exposure.

As anticipated, no fuel pin failures are predicted for the small-break cases during the first 60 s of the calculation. The small-break cases without pumped ECCS was subsequently extended to 393.0 s (at which time code failure occurred) for Oconee and to 1800.0 s for Seabrook, with no fuel failures predicted by either SCDAP/RELAP5/MOD3 or FRAP-T6.

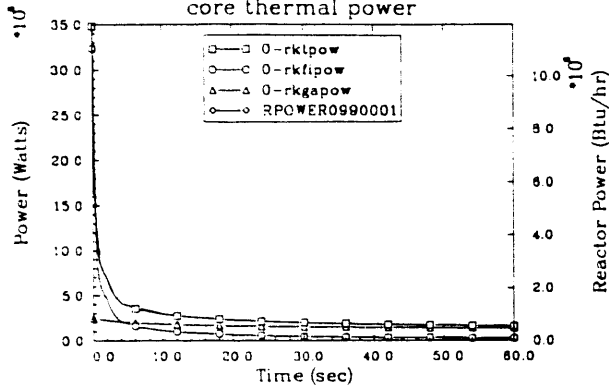
3.2 SUPPLEMENTAL TRAC-PF1/MOD1 CALCULATION

Figure 6 compares the transient results generated by SCDAP/RELAP5/MOD3 and TRAC-PF1/MOD1. The plots illustrate a good comparison of break flow and resulting system depressurization. The TRAC-PF1/MOD1 calculation reaches the low pressurizer pressure setpoint at 3.84 s, only 0.11 s later than indicated by the SCDAP/RELAP5/MOD3 calculation.^b The accumulator, intact hot leg, and cold leg flows also compare well.

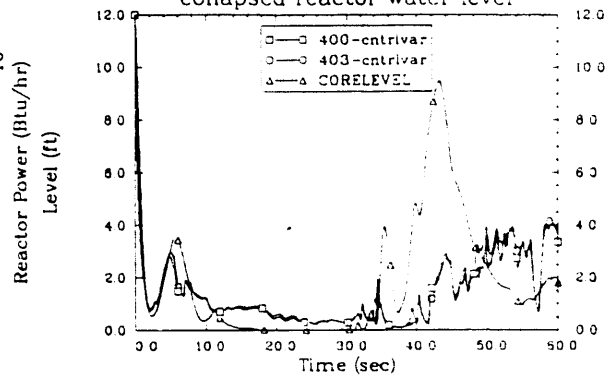
The largest deviation between results occurs after the accumulators empty and discharge nitrogen into the system. In the SCDAP/RELAP5/MOD3 calculation,

b. An additional delay of 2.0 s to account for instrument response is assumed for the analysis.

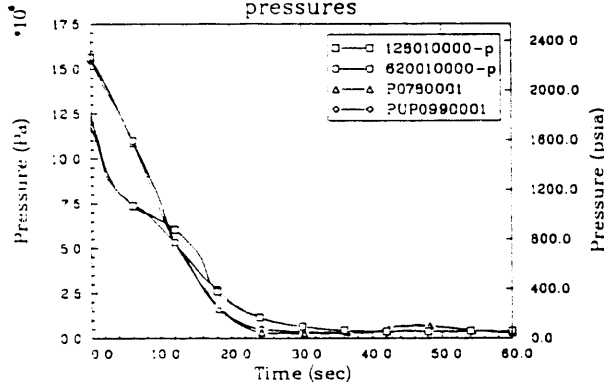
SEABROOK 100% DBA, TRAC-PF1 VS. RELAP5/MOD3
core thermal power



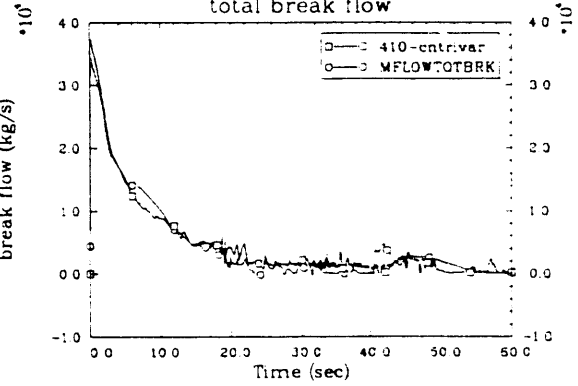
SEABROOK 100% DBA, TRAC-PF1 VS. RELAP5/MOD3
collapsed reactor water level



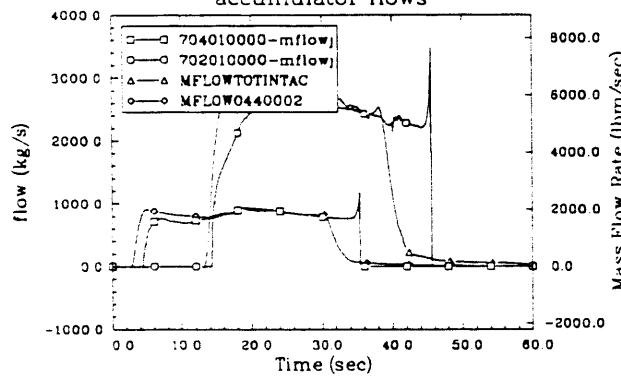
SEABROOK 100% DBA, TRAC-PF1 VS. RELAP5/MOD3
pressures



SEABROOK 100% DBA, TRAC-PF1 VS. RELAP5/MOD3
total break flow



SEABROOK 100% DBA, TRAC-PF1 VS. RELAP5/MOD3
accumulator flows



SEABROOK 100% DBA, TRAC-PF1 VS. RELAP5/MOD3
intact loop accumulator liquid volume

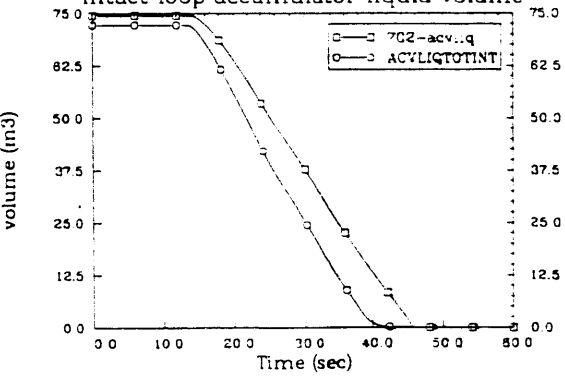
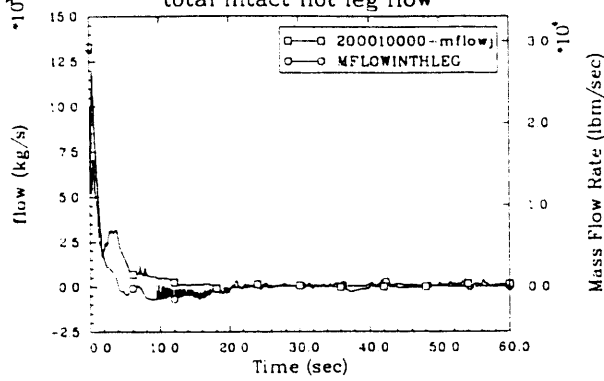
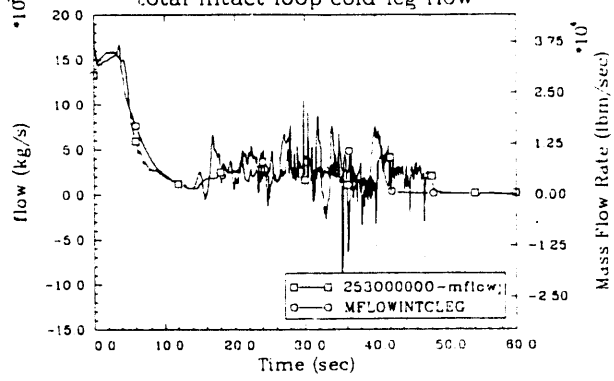


Figure 6. Plots of the transient results generated by SCDAP/RELAP5/MOD3 and TRAC-PF1/MOD1.

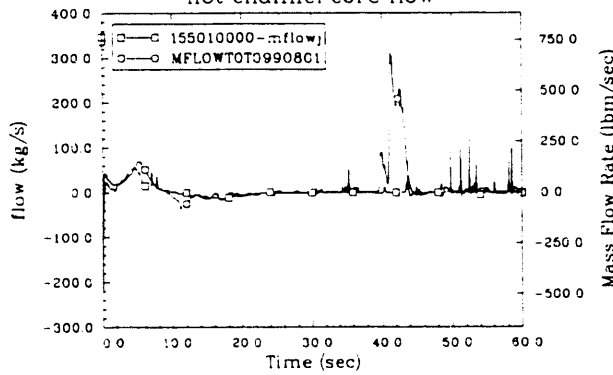
SEABROOK 100% DBA, TRAC-PF1 VS. RELAP5/MOD3
total intact hot leg flow



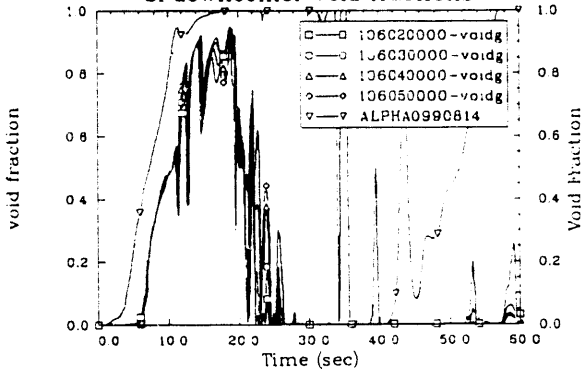
SEABROOK 100% DBA, TRAC-PF1 VS. RELAP5/MOD3
total intact loop cold leg flow



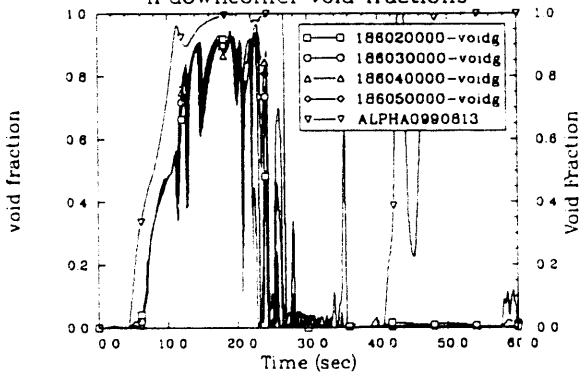
SEABROOK 100% DBA, TRAC-PF1 VS. RELAP5/MOD3
hot channel core flow



SEABROOK 100% DBA, TRAC-PF1 VS. RELAP5/MOD3
bl downcomer void fractions



SEABROOK 100% DBA, TRAC-PF1 VS. RELAP5/MOD3
il downcomer void fractions



SEABROOK 100% DBA, TRAC-PF1 VS. RELAP5/MOD3
time step size

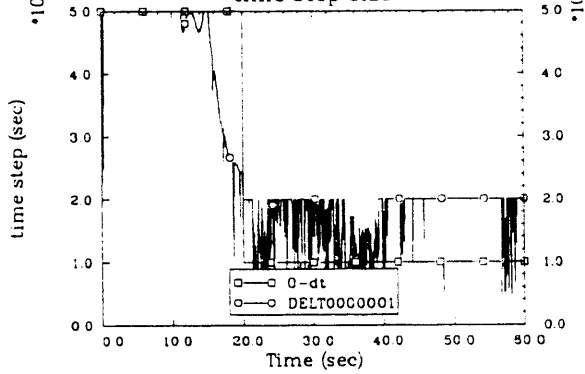


Figure 6. (continued)

| Variable | Description |
|-------------------------------------|---|
| SCDAP/RELAP5/MOD3 Variables: | |
| 0-rktpow | Total core thermal power (W) |
| 0-rkfipow | Total core fission power (W) |
| 0-rkgapow | Total core decay heat (W) |
| 400-cntrlvar | Hot channel collapsed reactor water level (m) |
| 403-cntrlvar | Core-average collapsed reactor water level (m) |
| 128010000-p | Reactor upper head pressure (Pa) |
| 620010000-p | Pressurizer dome pressure (Pa) |
| 410-cntrlvar | Total break flow (kg/s) |
| 704010000-mflowj | Accumulator flow for the broken loop (kg/s) |
| 702010000-mflowj | Total accumulator flow for the intact loop (kg/s) |
| 702-acvlig | Accumulator liquid volume for the intact loop (m ³) |
| 200010000-mflowj | Total hot leg flow for the intact loop (kg/s) |
| 253010000-mflowj | Total cold leg flow for the intact loop (kg/s) |
| 155010000-mflowj | Hot channel flows at the core midplane (kg/s) |
| 1060n0000-voidg | Broken loop downcomer void fraction for node n at the core midplane elevation |
| 1860n0000-voidg | Intact loop downcomer void fraction for node n at the core midplane elevation |
| 0-dt | Time step size (s) |
| TRAC-PF1/MOD1 Variables: | |
| RPOWER0990001 | Total core thermal power (W) |
| CORELEVEL | Core-average collapsed reactor water level (m) |
| PUP0990001 | Reactor upper head pressure (Pa) |
| P078001 | Pressurizer dome pressure (Pa) |
| MFLOWTOTBRK | Total break flow (kg/s) |
| MFLOW0440002 | Accumulator flow for the broken loop (kg/s) |
| MFLOWTOTINTAC | Total accumulator flow for the intact loop (kg/s) |
| ACQLIQTOTINT | Accumulator liquid volume for the intact loop (m ³) |
| MFLOWINTHLEG | Total hot leg flow for the intact loop (kg/s) |
| MFLOWINTCLEG | Total cold leg flow for the intact loop (kg/s) |
| MFLOWTOT990801 | Hot channel flows at the core midplane (kg/s) |
| ALPHA0990814 | Broken loop downcomer void fraction for node n at the core midplane elevation |
| ALPHA0990813 | Intact loop downcomer void fraction for node n at the core midplane elevation |
| DELTA0000001 | Time step size (s) |

Figure 6. (continued)

the accumulators were isolated as they approached an empty condition, in order to prevent code failure. In the TRAC-PF1/MOD1 calculation, however, as the accumulators empty, nitrogen gas is discharged into the cold leg and vessel. This surge of noncondensable gas pressurizes the upper downcomer, resulting in a surge of fluid into the core region. A surge can be seen as the broken loop accumulator empties at approximately 35 s and again as the intact accumulators empty at about 40 s. This surge of fluid is clearly seen in the hot channel mass flow at the midcore level. The downcomer void fraction plots indicate similar responses for voiding of the downcomer adjacent to the intact loops; however, the TRAC-PF1/MOD1 calculation indicates a quicker and more prolonged voiding of the downcomer quadrant adjacent to the broken cold leg.

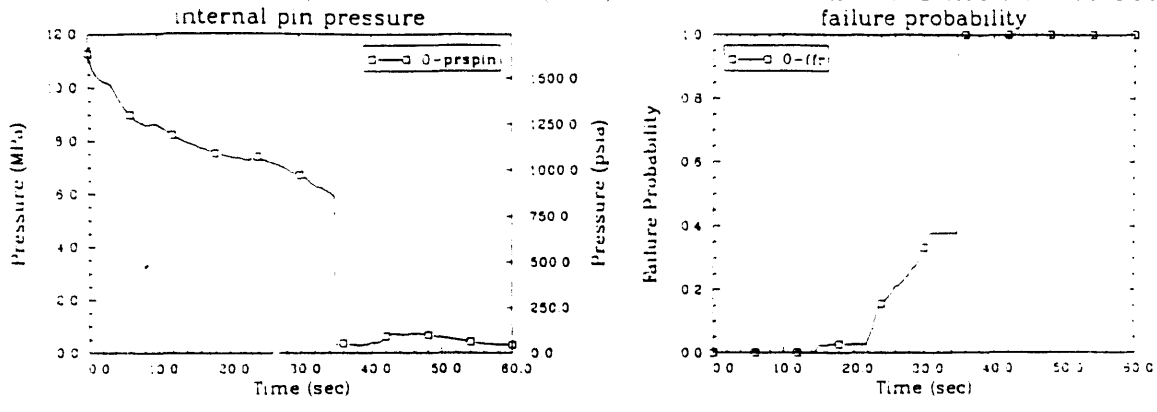
The FRAP-T6 fuel pin failure times generated using TRAC-PF1/MOD1 are summarized in Table 4. The axial node in which failure occurred is given in parentheses. The corresponding transient fuel performance results calculated by FRAP-T6 for a fuel pin operating with a power peaking factor of 2.32 and a peak burnup of 50 GWD/MTU are shown in Figure 7.

Table 4. Fuel pin failure times (s) calculated by FRAP-T6 using thermal-hydraulic conditions generated by TRAC-PF1/MOD1.

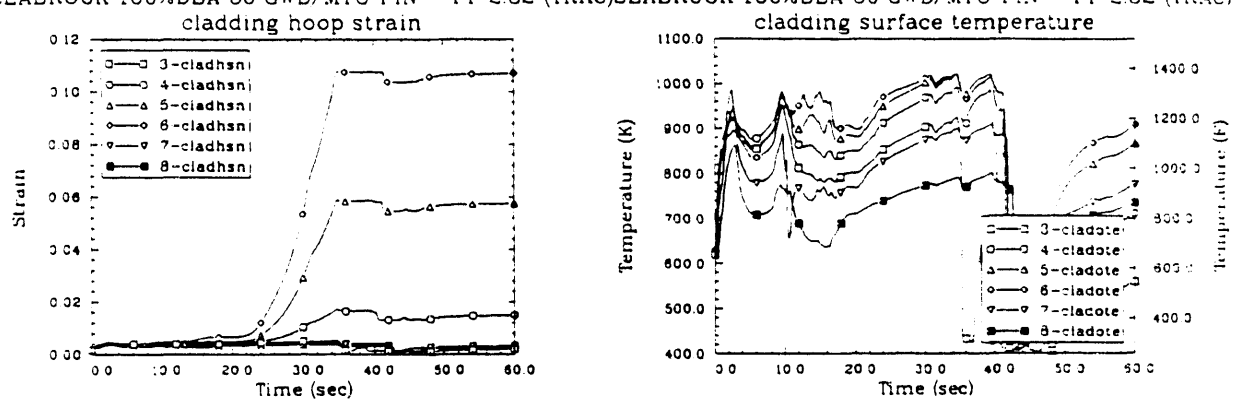
| Burnup/pf | 5 Gwd/MTU | 20 Gwd/MTU | 35 Gwd/MTU | 50 Gwd/MTU |
|-----------|-----------|------------|------------|------------|
| 2.32 | > 60.0 | 41.4 (5) | 41.3 (6) | 34.9 (6) |
| 2.2 | > 60.0 | > 60.0 | 41.4 (5) | 41.2 (6) |
| 2.0 | > 60.0 | > 60.0 | > 60.0 | > 60.0 |
| 1.8 | > 60.0 | > 60.0 | > 60.0 | > 60.0 |

Cladding surface temperatures calculated by FRAP-T6 using TRAC-PF1/MOD1 data are lower than those calculated using SCDAP/RELAP5/MOD3 data. As shown in Figure 7, this deviation becomes even more apparent after about 40 s, due to the

SEABROOK 100%DBA 50 GWD/MTU PIN--PF 2.32 (TRAC)SEABROOK 100%DBA 50 GWD/MTU PIN--PF 2.32 (TRAC)



SEABROOK 100%DBA 50 GWD/MTU PIN--PF 2.32 (TRAC)SEABROOK 100%DBA 50 GWD/MTU PIN--PF 2.32 (TRAC)



SEABROOK 100%DBA 50 GWD/MTU PIN--PF 2.32 (TRAC)SEABROOK 100%DBA 50 GWD/MTU PIN--PF 2.32 (TRAC)

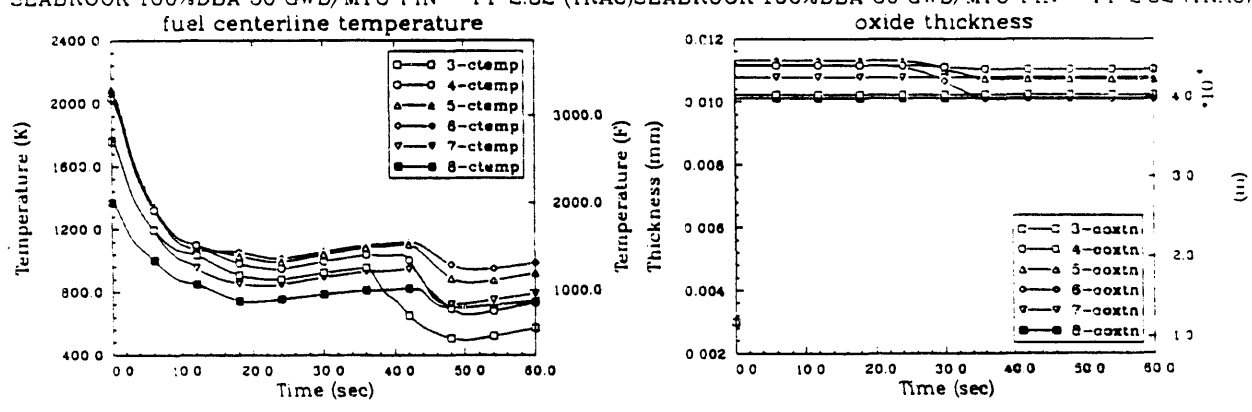


Figure 7. FRAP-T6 transient fuel performance results for the Seabrook hot channel hot pin, peaking factor 2.32, 50 Gwd/MTU burnup, using TRAC-PF1/MOD1 thermal-hydraulic boundary condition data.

nitrogen-induced flow surge that results in a quenching of the cladding for the TRAC-PF1/MOD1 calculation. In the TRAC-PF1/MOD1 case, pin failure occurs during the initial coolant surge, prior to reaching the phase transition temperature range. Based on this single TRAC-PF1/MOD1 calculation, the methodology using SCDAP/RELAP5/MOD3 to provide thermal-hydraulic boundary conditions for FRAP-T6 appears to produce conservative results (earlier fuel pin failure).

6. CONCLUSIONS

The earliest fuel pin failure times calculated for a complete, double-ended, offset-shear break of a cold leg, without pumped ECCS and assuming the main coolant pumps continued operating, are 13.0 s for Oconee using SCDAP/RELAP5/MOD3; 24.8 s for Seabrook using SCDAP/RELAP5/MOD3; and 34.9 s for Seabrook using TRAC-PF1/MOD1. The corresponding containment isolation signal times are 0.6, 3.73, and 3.84 s, respectively. A 2.0-s delay was assumed for instrument response. These values are summarized in Table 5, along with the minimum interval calculated between initiation of containment isolation and failure of the first fuel pin.

Table 5. Timing summary for worst-case LOCA runs using highest burnup and peaking factor results.

| Plant | Thermal-hydraulic model | Containment isolation (s) | Earliest pin failure (s) | Interval (s) |
|----------|-------------------------|---------------------------|--------------------------|--------------|
| Oconee | SCDAP/RELAP5/MOD3 | 2.6 | 13.0 | 11.4 |
| Seabrook | SCDAP/RELAP5/MOD3 | 5.7 | 24.8 | 19.1 |
| Seabrook | TRAC-PF1/MOD1 | 5.8 | 34.9 | 29.1 |

These values were obtained for fuel pins with the maximum discharge burnup, operating at the technical specification limits. This represents a conservative result, since fuel pins with such a high exposure would not be operating at such conditions. The fuel pin failure time can increase significantly for both lower burnup and lower peaking factor. An improved best-estimate approach would require detailed fuel-cycle-specific information on the core power and exposure distributions.

7. REFERENCES

1. *Code of Federal Regulations*, 10CFR Part 100, "Reactor Site Criteria," January 1, 1991.
2. G. A. Berna et al., *FRAPCON-2: A Computer Code for the Calculation of*

- Steady State Thermal-Mechanical Behavior of Oxide Fuel Rods*, NUREG/CR-1845, January 1981.
3. C. M. Allison et al. (Eds.), *SCDAP/RELAP5/MOD3 Code Manual*, NUREG/CR-5273, EGG-2555 (Draft), Revision 1, Volumes I-III, June 1990.
 4. L. J. Siefken et al., *FRAP-T6: A Computer Code for the Transient Analysis of Oxide Fuel Rods*, NUREG/CR-2148, May 1981.
 5. *TRAC-PF1/MOD1: An Advanced Best Estimate Computer Program for Pressurized Water Reactor Thermal-Hydraulic Analysis*, NUREG/CR-3858, April 1987.
 6. G. A. Berna, D. D. Lanning, and W. N. Rausch, *FRAPCON-2 Developmental Assessment*, PNL-3849, NUREG/CR-1949, June 1981.
 7. E. T. Laats, R. Chambers, and N. L. Hampton, *Independent Assessment of the Steady State Fuel Rod Analysis Code FRAPCON-2*, EGG-CAAP-5335, January 1981.
 8. L. J. Siefken, *Developmental Assessment of FRAP-T6*, EGG-CDAP-5439, May 1981.
 9. R. Chambers et al., *Independent Assessment of the Transient Fuel Rod Analysis Code FRAP-T6*, EGG-CAAD-5532, January 1981.
 10. Technical Program Group, *Quantifying Reactor Safety Margins: Application of Code Scaling, Applicability, and Uncertainty Evaluation Methodology to a Large-Break, Loss-of-Coolant Accident*, EGG-2552, NUREG/CR-5249, December 1989.
 11. D. M. Snider, K. L. Wagner, and W. Grush, *Nuclear Plant Analyzer (NPA) Reference Manual Mod-1*, EGG-EAST-9096, April 1990.
 12. J. E. Streit et al., *GRAFITI User Manual*, EGG-CATT-9604, March 1991.
 13. P. D. Bayless and R. Chambers, *Analysis of A Station Blackout Transient at the Seabrook Nuclear Power Plant*, EGG-NTP-6700, September 1984.
 14. P. D. Wheatley et al., *Evaluation of Operational Safety at Babcock and Wilcox Plants; Volume 2 - Thermal-Hydraulic Results*, NUREG/CR-4966, November 1987.
 15. Duke Power Co., *Final Safety Analysis Report, Oconee Nuclear Station Units 1, 2, and 3*, March 18, 1972.
 16. *Updated Final Safety Analysis Report, Seabrook Station*, May 26, 1989.
 17. D. A. Powers and R. O. Meyer, *Cladding Swelling and Rupture Models for LOCA Analysis*, NUREG-0630, April 1980.
 18. *Code of Federal Regulations*, 10CFR Part 50, Appendix K, "ECCS Evaluation Models," January 1, 1991.

NOTICE

This report was prepared as an account of work sponsored by an agency of the United States Government. Neither the United States Government nor any agency thereof, or any of their employees, makes any warranty, expressed or implied, or assumes any legal liability or responsibility for any third party's use, or the results of such use, of any information, apparatus, product or process disclosed in this report, or represents that its use by such third party would not infringe privately owned rights. The views expressed in this report are not necessarily those of the U.S. Nuclear Regulatory Commission.

END

**DATE
FILMED**

01 / 16 / 192

